



# The Influence of Dune Aspect Ratio, Beach Width and Storm Characteristics on Dune Erosion for Managed and Unmanaged Beaches

5 Michael Itzkin<sup>1</sup>, Laura J. Moore<sup>1</sup>, Peter Ruggiero<sup>2</sup>, Sally D. Hacker<sup>3</sup>, and Reuben G. Biel<sup>1</sup>

<sup>1</sup>Department of Geological Sciences, University of North Carolina, 104 South Road, Mitchell Hall, Campus Box 3315, Chapel Hill, North Carolina 27515, USA

<sup>2</sup>College of Earth, Ocean, and Atmospheric Sciences, Oregon State University, 104 CEOAS Administration Building, Corvallis, OR 97331, USA

10 <sup>3</sup>Department of Integrative Biology, Oregon State University, 3029 Cordley Hall, Corvallis, OR 97331, USA

*Correspondence to:* Michael Itzkin ([mitzkin@unc.edu](mailto:mitzkin@unc.edu))

**Abstract.** Dune height is an important predictor of dune impact during a storm event given that taller dunes have a lower likelihood of being overtopped. However, the temporal dominance of the wave collision regime, wherein significant volume loss (erosion) from the dune will occur through dune retreat without the dune being overtopped, suggests that dune width must also be considered when evaluating the vulnerability of dunes to erosion. We use XBeach, a numerical model that simulates hydrodynamic processes, sediment transport, and morphologic change during a storm, to analyze dune erosion as a function of dune aspect ratio (i.e., dune height versus dune width) for storms of varying intensity and duration. We find that low aspect ratio (low and wide) dunes lose less volume than high aspect ratio (tall and narrow) dunes during longer storms, especially if they are fronted by a narrow beach. During more intense storms, low aspect ratio dunes experience greater erosion as they are more easily overtopped than high aspect ratio dunes. In managed scenarios where sand fences are used to construct a “fenced” dune seaward of the existing “natural” dune, we find that the fenced dune effectively prevents the natural dune behind it from experiencing any volume loss until the fenced dune is sufficiently eroded, reducing the magnitude of erosion of the natural dune by up to 50%. We also find that beach width exerts a significant influence on dune erosion; a wide beach offers the greatest protection from erosion in all circumstances regardless of dune morphology or storm characteristics. These



findings suggest that efforts to maintain a wide beach may be effective at protecting coastal communities from dune loss. However, in maintaining wide beaches and dunes, the protection offered in the short-term must be considered against long-term detrimental effects of potentially limiting overwash fluxes, which are critical to maintaining island elevation as sea level rises.

## 1. Introduction

Foredunes provide the first line of defense for coastal communities against overwash and inundation during storms. To this end, a tall dune is often considered ideal for mitigating storm impacts as its height is less likely to be exceeded by the storm-induced total water level (TWL) (Biel et al., 2017; Sallenger, 2000; Seabloom et al., 2013; Stockdon et al., 2006). Considering that wave runup is most likely to impact the dune face (i.e., collision; Sallenger, 2000)—which is more likely to affect the width of the dune rather than the height—is the most temporally common impact regime during a storm (Brodie et al., 2019; Stockdon et al., 2007), the width of the dune is an important predictor of how much erosion a dune might experience during a storm. While dune height change is an important metric to consider when measuring storm impacts (e.g., Long et al., 2014), other measures of dune erosion, such as volume loss (e.g., Durán et al., 2016; Larson et al., 2004), may better describe the overall change in morphology by accounting for changes in height as well as width (Figure 1). Understanding how the relative value of height divided by width, or aspect ratio, in foredune morphology will affect storm-induced erosion and impacts to coastal communities is important, especially because pre-storm dune shape is affected by both environmental and anthropogenic processes.

Dunes form as a result of biophysical feedbacks between aeolian sediment transport and vegetation growth (Duran and Moore, 2013; Hesp, 2002; Houser et al., 2015; Maun, 1998; Stallins and Parker, 2003). The cross-shore position and height of the dune are controlled by the distance between the shoreline and the seaward limit of vegetation, with larger distances typically being associated with the formation of taller dunes (Duran and Moore, 2013; Hesp, 2002). While vegetation zonation controls the positioning and height of the dune, the dominant plant species can influence overall dune shape (e.g., Biel et al., 2019; Hacker et al., 2012; Woodhouse et al., 1977; Zarnetske et al., 2010, 2012). Dune grasses that tend to grow more horizontally than vertically will form dunes that are shorter and wider, and vice-versa. For example, Hacker et al. (2012) found that dunes in the Pacific Northwest (PNW) formed in the presence of *Ammophila arenaria* were typically taller and narrower than dunes formed in the presence of



55 *Ammophila breviligulata*. *Ammophila arenaria* grows more vertically while *A. breviligulata* grows more laterally and  
their respective dune morphologies reflect that difference. As a result, coastal foredunes in the PNW where *A.*  
*breviligulata* is dominant may be exposed to a greater risk of overtopping (Seabloom et al., 2013). In a study of east  
coast dune grass species (*A. breviligula* and *Uniola paniculata*), Woodhouse (1977) found that dunes formed in the  
presence of *A. breviligulata* were shorter and wider than those formed in the presence of *U. paniculata* under similar  
60 environmental conditions; a result confirmed by the recent work of Hacker et al. (2019) and Jay et al. (in review).

In addition to natural controls on dune growth and dune shape, human modifications to the beach and dune  
system typically involve constructing a new foredune, or fortifying the existing foredune to make it more resistant to  
erosion (e.g., Elko et al., 2016; Nordstrom et al., 2000; Nordstrom & Jackson, 2013), often through the use of sand  
fencing (e.g., Anthony et al., 2007; Charbonneau & Wnek, 2016; Jackson & Nordstrom, 2018; Miller et al., 2001). In  
65 a study on the geomorphic effects of sand fencing, Itzkin et al. (2020) demonstrated that foredunes are lower in  
elevation in areas where sand fences are constructed but that the dune system is substantially wider than foredunes in  
areas without sand fences. Other management decisions, such as allowing vehicles to drive on beaches and beach  
raking, can also bring forth tradeoffs between dune growth and coastal protection (Defeo et al., 2009). In a study on  
the effects of dune grass removal to restore Western snowy plover habitats in the PNW, Biel et al (2017) used XBeach  
70 (Roelvink et al., 2009) to explore dune erosion and found that where beachgrasses were removed, dunes maintained a  
lower elevation and were predicted to be more vulnerable to erosion compared to foredunes where beachgrasses were  
not removed and grew to a stable elevation. Beach nourishment may also be used to widen the beach (and decrease  
its slope), limiting wave impacts to the dune and stimulating dune growth (e.g., Cohn et al., 2019; van Puijenbroek et  
al., 2017; Ruggiero et al., 2001, 2004).

75 The main goal of the work presented here was to assess how foredunes of varying aspect ratios aspect ratio  
(i.e., low and wide to tall and narrow foredunes) are eroded as a function of storm duration and total water level  
(TWL). We used the numerical model XBeach (Roelvink et al., 2009), which is a process-based numerical model  
that simulates the hydrodynamics and morphodynamics in the nearshore over storm time scales as well as sediment  
transport and morphologic changes to the dune and has been well validated for simulating dune response to storms  
80 (e.g., Cohn et al., 2019; McCall et al., 2010; Vousdoukas, Ferreira, Almeida, & Pacheco, 2012) to address the  
following questions. (1) How does storm duration affect volumetric dune erosion as a function of foredune aspect  
ratio? (2) How do variations in storm TWL affect volumetric dune erosion as a function of foredune aspect ratio? (3)



How does the morphology of the beach (i.e., width and slope) affect volumetric dune erosion independent of foredune aspect ratio. We also compare our model results with observed pre- and post-storm lidar and field profiles from the North Carolina coast to ground-truth our analyses.

## 2. Methods

### 2.1 Beach and Foredune Morphometrics

To track changes in dune and beach morphology throughout our simulations, the following morphometrics are calculated at every model time step: dune aspect ratio, dune volume, overwash volume, and beach width. The dune aspect ratio was calculated as the height of the natural dune from  $D_{\text{high}}$  to  $D_{\text{low}}$  divided by the width of the dune from  $D_{\text{heel}}$  to  $D_{\text{toe}}$  (Figure 1). The dune volume is calculated by integrating over the portion of the profile contained within the original cross-shore location of the dune ( $D_{\text{low}}$  to  $D_{\text{heel}}$ ) in the first-time step and above the  $D_{\text{low}}$  elevation (0.59 m, NAVD88). The overwash volume is similarly calculated as the change in volume of the profile landward of the initial  $D_{\text{heel}}$  position. Finally, the beach width is calculated as the cross-shore distance between MHW and  $D_{\text{low}}$  at every time step. Given that  $D_{\text{low}}$  was held constant across all simulations, the beach slope is inversely proportional to the beach width in our simulations (i.e., beach slope decreases as beach width increases).

### 2.2 Observed Foredune Profiles

We use changes between in situ beach profiles from 2017-2018, which capture the influence of Hurricane Florence, to test model results. Topographic profiles were measured along Bogue Banks, NC, USA (BB) using a Trimble Real Time Kinematic Global Positioning System (RTK-GPS) in October of 2017 and 2018. Twenty-two total profiles were surveyed with an alongshore spacing of 1-2 km. For each field transect, we calculate the aspect ratio, beach width, and dune volume using the methods described above.

We also use BB as a reference location for developing model inputs and synthetic dune profiles (described in sections 2.3-2.5). BB is a roughly 40 km long developed barrier island in the Outer Banks of North Carolina whose dune system has been modified through the use of sand fencing which has led to the development of a low-wide dune where the fences are present. We use a profile from Fort Macon, a non-fenced portion of the island, as a reference location for a typical “natural” dune shape for our modelled synthetic dunes.

### 2.3 Synthetic Dune Profiles

We created a set of synthetic beach-dune profiles using a LiDAR-derived initial reference profile from Fort Macon, North Carolina, USA (Figure 2). We fit an exponential curve to a measured bathymetric profile in order to



extend the beach profile to the buoy depth of 30.5 m. The height of the reference dune was increased (decreased) in 20% intervals as:

$$H_f = H_r * \left(1 - \frac{stretch}{100}\right) \quad (1)$$

where  $H_f$  is the post-stretch dune height,  $H_r$  is the height of the reference dune, and stretch is a multiple of 20 between 115 -60 and 60. Every increase (decrease) in dune height is paired with a decrease (increase) in dune width such that:

$$W_f = \frac{W_r}{1 - \frac{stretch}{100}} \quad (2)$$

where  $W_f$  is the post-stretch dune width,  $W_r$  is the reference dune width. This method of simultaneously modifying dune height and width allowed for dune volume to be conserved (and therefore essentially held constant across simulations) and resulted in a suite of beach profiles with aspect ratios (i.e., dune height divided by dune width) 120 ranging from 0.02 to 0.27 and dune volumes between 50.6 and 53.5 m<sup>3</sup>/m.

We adjusted the position of the dune on the profile to create four different cross-shore configurations: 1) dune toe ( $D_{low}$ ) positions aligned, 2) dune crest ( $D_{high}$ ) positions aligned, 3) dune heel ( $D_{heel}$ ) positions aligned, and 4) dune toe ( $D_{low}$ ) positions aligned with a sand-fenced dune seaward of it (Figure 2A-D). Simulations with the  $D_{low}$  position aligned ensured that all dunes share the same beach morphology, thereby controlling for the effects of beach slope on 125 wave runup (i.e., Stockdon et al., 2006). Simulations with the  $D_{high}$  positions aligned may be more representative of a more natural setting in which wider beaches are backed by taller dunes. Simulations with  $D_{heel}$  positions aligned may be more representative of a managed shoreline, where the dunes are widened seaward and thus share a common heel position regardless of dune height. In both the  $D_{high}$  and  $D_{heel}$  aligned scenarios, the beach width increases proportionally to the aspect ratio of the dune. The fourth configuration (Figure 2D) represents a dune complex that 130 arises when sand fences are placed on managed shorelines. The fenced profiles consist of the dune profiles in which the  $D_{low}$  position was aligned (Figure 2A) and the addition of a gaussian curve on the seaward side of the dune to represent a typical fenced dune shape (Itzkin et al., 2020).

To demonstrate that the synthetic dunes are consistent with observed morphologies, and that it is reasonable to hold the volume constant for a dune while modifying its aspect ratio, we compared the aspect ratios and volumes 135 of the synthetic dune profiles with those of LiDAR-derived dune profiles from Bogue Banks measured between 1997 and 2016 (Figure 3). The aspect ratios of dunes on Bogue Banks range up to approximately 1.08 and 89.4% of all profiles fall within the range of aspect ratios of our synthetic profiles. While all of the lidar data is extracted in locations where dunes are present, the lowest aspect ratios explored in this study are essentially flat, representing conditions in



140 which a dune is absent. Dune volumes on Bogue Banks range up to 350 m<sup>3</sup>/m with the modelled value representing the 80<sup>th</sup> percentile. Given the relatively weak relationship between dune volume and dune aspect ratio (with the aspect ratios used in this study having a wide range of associated volumes; Figure 3), maintaining a relatively constant dune volume while varying the dune aspect ratio in our model simulations is reasonable.

#### 2.4 Synthetic Storm Hydrographs

145 We created a set of synthetic storms for use in the model simulations by using Hurricane Matthew as a reference storm and then increasing its duration by up to 48 hours (Figure 4). Hurricane Matthew moved northward along the North Carolina coast on the afternoon of October 8, 2016, generating approximately 1 m of storm surge and significant wave heights (Hs) of approximately 7.5 m. To capture the full spin up, peak, and relaxation of the storm, we used wave (Hs, Tp, Direction) and tide data for October 7-10, 2016, from the nearest NOAA National Data Buoy Center (NDBC) buoy (41159; Onslow Bay, NC; depth = 30.5 m) and NOAA tide gauge (Station CLKN7; Beaufort, 150 NC). We used linear wave theory to transform the wave parameters to the 30.5 m depth contour to account for shoaling and refraction with the transformed wave data used as input for XBeach.

To represent a longer duration storm than the base storm, we used the Hurricane Matthew storm time series to identify a 12-hour window centered on the timing of peak storm surge. We then interpolated all hydrodynamics (i.e., Hs, Tp, direction, and SWL) within this temporal window onto a +12hr, +18hr, +24hr, +36hr, and +48hr temporal 155 “grid,” effectively increasing the storm’s duration by up to two days. We held constant the spin up (rising hydrograph) and relaxation (falling hydrograph) of the storm for all simulations. For all storm durations, we created a version in which the surge is unmodified (1.0x), decreased by 50% (0.5x), and increased by 50% (1.5x). In total, this yielded 18 different synthetic storms (Figure 4).

The duration of our synthetic storms varied from 73 hr to 122 hr, and the surge in our synthetic storms varied 160 from ~0.5 m to ~1.25 m. This compares favorably to other storms that have recently affected the North Carolina coast, including Tropical Storm Joaquin (duration ~144 hours) and Hurricane Florence (Duration ~48 hours) (Figure 5). Water levels during Tropical Storm Joaquin were elevated for 6 days, which is comparable to the total duration of the +48 hr storm time series. Peak surge during Hurricane Florence was ~1.6 m, a similar order of magnitude to the maximum storm surge we used in the synthetic time series.

#### 165 2.5 Foredune Erosion Simulations



We used the XBeach (Roelvink et al., 2009) model to simulate the effects of the synthetic storms described in Section 2.2 on the profiles described in Section 2.1. We ran XBeach (version 1.23.5465) in 1D-hydrostatic mode with the break parameter set to roelvink\_daly and the gamma parameter set to 0.52 to better capture the effect of swash processes on the reflective beach profiles (Roelvink et al., 2018) and all other parameters left to their default setting.

170 The profiles described in Section 2.1 were gridded for use with XBeach with a 1m subaerial spacing and a varying 5-20 m subaqueous spacing to decrease computational cost.

We grouped the simulations into 12 “experiments” that encompass all combinations of dune configuration (i.e., toes-aligned, crests-aligned, heels-aligned, and fenced) and storm surge modification (i.e., 0.5x, 1.0x, 1.5x) (Figure 6). Within each experiment, we factorially simulated all combinations of dune aspect ratios and storm

175 durations, which resulted in a total of 504 simulations (12 experiments with 42 simulations per experiment). We note that all dune erosion experienced during the simulations occurred in the collision regime (Sallenger, 2000), unless stated otherwise. Further, fenced profiles do not contain any structural reinforcement from a fence being present that might limit how the dunes are eroded; although the fenced dune itself limits erosion of the natural dune behind it, the authors are unaware of any studies showing an effect on dune erosion during a storm from the fence itself.

### 180 3. Modelling Results

#### 3.1 Erosion on Synthetic Dunes

Overall, our simulations for dunes without fences showed that losses in foredune volume were greater with higher storm surges, longer storm durations, or when dunes are located closer to the shoreline (represented by the dune toes-aligned scenarios; Figure 7). Under most simulated conditions, foredunes eroded except when they had a high

185 dune aspect ratio, situated farther from the shoreline (dune heels-aligned), and the storm was of low intensity, in which case there was slight accretion at the dune toe due to wave processes (Figure 7). Below are the specific results of the erosion simulations using the three cross-shore synthetic dune configurations.

##### 3.1.1 Dune Toes Aligned

Simulations with the dune toes aligned showed that there was greater erosion for the high-aspect ratio dunes

190 compared to the low-aspect ratio dunes (Figure 7A, E, I). The heightened erosion was especially acute with low intensity storms where there was a  $\sim 20$  m<sup>3</sup>/m ( $\sim 38\%$ ) difference in volume loss between the high and low-aspect ratio dunes. For the most intense storms, the difference in volume loss between the high and low-aspect ratio dunes was  $\leq 10$  m<sup>3</sup>/m ( $\sim 19\%$ ). As expected, increasing the duration of the storms led to an increase in the amount of overall



erosion experienced, especially for high-aspect ratio dunes. For example, for the longest storms (+48 hr) with a  
195 moderate intensity, high aspect ratio dunes experienced complete erosion from extended scarping until the dune  
collapsed (Figure 7E). For the longest storms with the greatest intensity, all of the dunes experience inundation  
regardless of aspect ratio (Figure 7I).

### 3.1.2 Dune Crests Aligned

Simulations with the dune crests aligned showed a more typical pattern of erosion for which the low-aspect  
200 ratio dunes consistently experienced greater volume loss than the high-aspect ratio dunes (2-3x depending on storm  
duration; Figure 7B, F, J). In these simulations, the low-aspect ratio dunes experienced a greater sensitivity to increases  
in storm intensity and storm duration. As surge intensity increased (0.5x to 1.5x surge scenarios), volume loss from  
the high-aspect ratio dunes increased by up to  $\sim 20 \text{ m}^3/\text{m}$  ( $\sim 38\%$ ) while volume loss from the low-aspect ratio dunes  
increased by up to  $\sim 30 \text{ m}^3/\text{m}$  ( $\sim 58\%$ ) (Figure 7B,F, J). Similar increases in volume loss were observed as storm  
205 duration increased from the base scenario to the +48 hour scenario. In simulations with the crests aligned, inundation  
only occurred for low-aspect ratio dunes during the longest, most-intense storms (Figure 7J).

### 3.1.3 Dune Heels Aligned

Simulations with the dune heels aligned showed similar erosional trends as the simulations with the dune  
crests aligned but with a lower overall quantity of volume loss (Figure 7C, G, K). During the lowest intensity storms,  
210 moderate-to-high aspect ratio dunes did not experience any volume loss and even the low-aspect ratio dunes did not  
significantly erode until storm duration reached +18 hours. While erosion increased for all dunes with increasing  
intensity and duration of the storm, moderate-to-high aspect ratio dunes consistently experienced  $\sim 50\%$  less volume  
loss than the low-aspect ratio dunes (Figure 7C, G, K). Similar to the dune crests-aligned simulations, complete dune  
erosion only occurred for low-aspect ratio dunes during the longest and most-intense storms (Figure 7K).

## 215 3.2 Erosion of Synthetic Dunes with Sand Fences

We performed a suite of simulations using the same dune profiles as the dune toes-aligned scenarios but with  
a portion of the beach replaced by a fenced dune (Figure 1D). We found that dune erosion increased with both storm  
duration and storm intensity (Figure 7D, H, L). However, the aspect ratio of the dune behind the fence plays a minimal  
role in influencing volume loss except in the case of the most intense storms, when the fenced dune is inundated and  
220 the dune behind it begins to experience impacts from wave runoff (Figure 7D, H, L). The dunes behind the fenced



dunes were only inundated during the longest, most-intense storms (Figure 7L). Overall, the trends in erosion from fenced scenarios showed a systematic decline in erosion of up to 50% compared to the unfenced scenarios.

In addition to sand volume lost from the dune, we calculated the overwash volume as the difference in sand volume behind the dune after the storm. Differences in overwash volume between the fenced and unfenced scenarios are only relevant when overwash/inundation are experienced. Thus, under low storm intensity scenarios, overwash volume is zero. For moderate intensity storms, only the unfenced natural dunes experienced inundation, resulting in a positive difference in overwash volume between the fenced and unfenced simulations (Figure 8A). For the most intense storms up to  $\sim 50 \text{ m}^3/\text{m}$  more overwash volume is experienced by the dunes without fences (Figure 8B).

### 3.3 Beach Width Effects on Dune Erosion

Given that wave runup and erosion during a storm is lower for wider, more gently sloping beaches (i.e., Ruggiero, Holman, & Beach, 2004; Stockdon et al., 2006; Straub et al., 2020), we were interested in analyzing the separate effects of beach width on dune erosion (Figure 9). In particular, for dunes in which dune toes are aligned, beach width would be held constant for all aspect ratios and thus would not affect the outcome for erosion. However, because crest and heel aligned dunes can vary in their beach morphology depending on aspect ratio, this difference leads to wider beaches and might explain decreased erosion for high aspect ratio dunes. We also note that because the dune toe elevation is consistent across simulations, the beach width is inversely related to the beach slope in our simulations.

In all the simulations, regardless of dune configuration, there was a significant decrease in the amount of erosion as the width of the beach increased (Figure 9). For example, for any given beach width, the dune volume loss was similar in both the crests-aligned and heels-aligned scenarios despite the variability in dune morphology. Additionally, the sensitivity of the dune to decreases in storm duration was inversely proportional to the beach width such that dunes fronted by wide beaches were noticeably less sensitive to increases in storm duration than dunes fronted by narrow beaches (Figure 9). This same trend was observed when analyzing increases in storm intensity; the increase in dune volume loss as surge elevation increased is much less in the cases of wider beaches (Figure 9). All of the dunes that were completely inundated (Figure 7) were fronted by narrow beaches during long, intense storms (Figure 9).

### 3.4 Simulation Comparisons with Field Surveys



We compared our model results to the observational field surveys that were conducted along Bogue Banks, NC, before (2017) and after (2018) Hurricane Florence. The field data showed a weak relationship between dune aspect ratio and erosion (sand volume loss). However, similar to model results for the toes-aligned (constant beach width) dune configurations, those profiles with a lower aspect ratio dune experienced similar or even less erosion than high aspect ratio dunes with the same beach width (i.e., at a beach width of 40 m in Fig. 10). A strong trend is seen with respect to the beach width, in which erosion significantly decreased with increasing beach width, regardless of aspect ratio (Figure 10). Foredunes with beach widths greater than 40 m all experienced dune growth between 2017-2018 despite the effects of Hurricane Florence during this period (Figure 10). Although the model does not simulate aeolian transport induced dune growth, we note that in simulations with low to moderate surge (0.5x-1.0x), sand volume loss decreased to zero or near-zero for beach widths greater than 40m (Figure 9, heels-aligned).

#### 4. Discussion

##### 4.1 Effects of Aspect Ratio on Dune Erosion

The storm impact scale for barrier islands described by Sallenger (2000) relates the elevation of the dune crest and dune toe to TWL as a means of categorizing impacts within the four possible wave impact regimes: swash, collision, overwash, and inundation. Each wave impact regime has a corresponding mode of beach and dune erosion associated with it from none (swash) to potentially complete loss of the dune (inundation). A key implication of this wave impact scale is that a taller dune should provide better protection from storms as it is less likely to be overtopped. Previous studies (e.g., Brodie et al., 2019; Stockdon et al., 2007) have suggested that collision is the most common, but temporary, wave impact regime experienced by foredunes. Collision occurs when the total water level impacts the face of the dune, causing scarping and dune retreat. This suggests that a dune which is more resistant to the effects of collision may offer the greatest degree of protection so long as it is not overtopped, especially given that the dune will likely be experiencing collision for a longer time under longer duration storm events.

When controlling for the beach width (i.e., the dune toes-aligned scenario), we find that the lower aspect ratio dunes eroded less than the higher aspect ratio dunes when both are in the collision regime. The high aspect ratio dunes are more likely to collapse when scarped because of avalanching as the dune face slope approaches an angle of repose, this also explains the accretion at the dune toe for the high aspect ratio dunes that weren't completely eroded through (Palmsten and Splinter, 2016). Using a Bayesian Network Biel et al. (2019) found that the dune face slope is a strong predictor of vertical dune erosion for similar reasons, demonstrating the importance of storm duration and the effects



of wave collision duration when considering how a dune is likely to erode. Although the high aspect ratio dunes are more equipped to prevent overwash, there is the potential for them to be completely eroded during the longest storms due to persistent scarping, undercutting, and avalanching. In contrast, low aspect ratio dunes can withstand long duration storms as long as the surge is not high enough in elevation to cause overwash. While the height of the dune  
280 may be an appropriate predictor for overwash, the overall aspect ratio may better describe how dunes will erode with respect to storm duration and intensity.

#### 4.2 Sand Fences and Beach Nourishment on Foredune Erosion

We assessed the effects of sand fencing on the mitigation of dune erosion by comparing the results of the fenced and unfenced simulations. We found that the small dune formed by fencing can significantly decrease dune  
285 erosion by providing a barrier that must be eroded away before the dune itself is impacted. In our simulations, the fenced dune was not eroded through until ~60 hrs into the storm, which prevented the dune behind it from experiencing the peak of the storm (Figure 4). The foredune behind the fenced dune was only inundated during the longest and most intense storms, as opposed to the dunes without fences, which experienced inundation during the moderate (1.0x surge) intensity storms (Figure 7). The key dynamic in this case (regardless of actual storm duration), was that the  
290 fenced dune was sufficiently high to protect the natural dune until the peak of the storm had passed. The foredune behind a fenced dune is not impacted until the fenced dune is eroded away, making the aspect ratio of the foredune secondary to the morphology of the fenced dune in providing protection to back-barrier environments. Charbonneau and Wnek (2016) demonstrated that fenced dunes can reform quickly (on the order of months) meaning that not only do sand fences effectively prevent storm-induced erosion, but it is possible for them to facilitate recovery- of the  
295 fenced dune prior to the next storm if the frequency of storm impacts is sufficiently low, and assuming the fences are still present following the storm or are re-built. Additionally, dunes built by sand fences may be paired with vegetation planting to assist in sand trapping efficiency and dune stabilization (Bossard and Nicolae Lerma, 2020; Nordstrom and Jackson, 2013).

We also considered the effect of beach nourishment by varying beach width for the dune crest-aligned and  
300 dune heels-aligned scenarios. For a given dune aspect ratio, the only difference between the toes-aligned, crests-aligned, and heels-aligned simulations was the beach width, which increased from the dune toes to dune heels-aligned simulations. Beach nourishment appears, from model results, to have a greater impact on preventing dune erosion than any action that could be taken to alter the aspect ratio of the dune. XBeach simulations with the dune crests and heels-



aligned have a variable beach width that is proportional to the dune aspect ratio. For a given dune aspect ratio and  
305 wave duration and intensity, the only difference between the simulations is the increase in beach width (toes-aligned  
< heels-aligned). By increasing the width of the beach, the slope of the beach ( $\beta_t$ ) is decreased, which lowers incident  
band swash (e.g., Ruggiero et al., 2004) and total wave runup (Stockdon et al., 2006), reducing the likelihood of dune  
erosion. We see this effect in our results, which show up to a 100% reduction in dune erosion between the toes and  
heels-aligned simulations (Figure 7). The strong inverse relationship between beach width and dune erosion (Figures  
310 9 and 10) suggests that regardless of the aspect ratio of a foredune, widening the beach can be sufficient for preventing  
overwash during most storms and will be a more effective strategy for increasing coastal protection than re-building  
the dune or installing sand fences.

It is important to recognize that although management initiatives such as widening beaches and building  
dunes with particular aspect ratios can be effective at mitigating erosion, they have long-term effects that are worth  
315 considering. Even though this study considers individual storm events, the difference in erosion due to overwash for  
the fenced and unfenced dunes (Figure 8) have clear implications for barrier island vulnerability. Overwash facilitates  
barrier rollover, a necessary process for the island to maintain subaerial exposure as sea level rises (e.g., Leatherman,  
1979; Moore et al., 2010; Lorenzo-Trueba & Ashton, 2014; Rogers et al., 2015). The large decrease in overwash  
volume in our fenced simulations suggests that rollover may be inhibited in managed locations, thereby increasing the  
320 likelihood of eventual barrier drowning (e.g., Magliocca et al., 2011; Rogers et al., 2015).

## 5. Conclusions

In this study we analyzed how coastal foredunes erode as a function of their aspect ratio, whether they have  
fencing, and the width of their beaches as a result of beach nourishment. We find that low aspect ratio (lower and  
wider) dunes are more resistant to erosion from increased storm duration than high aspect ratio (taller and narrower)  
325 dunes, although high aspect ratio dunes offer greater protection against more intense storms. For low aspect ratio  
dunes we typically observe complete erosion of the dune through inundation (Sallenger, 2000) during long duration  
storms with a high surge, whereas the high aspect ratio dunes are completely eroded away through persistent scarping  
during the longest storm events until the dune is low enough to be overtopped. In addition, dunes built by sand fences  
reduced the amount of erosion experienced by the foredune behind the fenced dune because they create a barrier that  
330 must first be eroded or overtopped. Although modifying the dune aspect ratio does alter the amount of erosion



experienced as storm characteristics vary, we find that the greatest protective service in all instances is offered by a wide beach; a finding that also supported by existing foredunes in the field.

The configuration that would offer the greatest protection from erosion and inundation would be a tall, wide foredune fronted by a wide beach with a fenced dune. Given the challenges of achieving such a foredune morphology in the face of rising sea level and within resource limitations (i.e., sand availability, cost, etc.), our findings suggest that the greatest increase in protective service can be achieved by widening beaches, regardless of the frontal dune morphology. Although our work demonstrates that widening a beaches through nourishment may provide more protection from flooding in the short-term than artificially constructed dunes, it is costly and may be infeasible over the long-term in the face of sea level rise and shoreline erosion, thus managed retreat may be a more viable for strategy for widen beaches (e.g., Cutler et al., 2020; Gibbs, 2016). Further, dune building initiatives, such as the emplacement of sand fences, that increase the width of the dune, likely offer the greatest protection against longer storms. Though wider dunes do not necessarily decrease the likelihood of overwash, given that wave collision is a common and frequent mode of dune erosion (e.g., Brodie et al., 2019), a wider dune does provide protection from the most commonly experienced mode of erosion. Though potentially beneficial in the short-term, widening beaches and reducing overwash through the emplacement of tall dunes can also have negative long-term consequences because they reduce overwash flux, which is essential for barrier islands to maintain elevation as sea level continues to rise (i.e., Lorenzo-Trueba & Ashton, 2014; Magliocca et al., 2011; Rogers et al., 2015). Ultimately, pairing wide dunes and wide beaches to provide protection from the most common storm scenarios may balance the need for protection from most storms, but this must be considered against a longer-term need for the island to rollover and maintain a subaerial surface via overwash processes lest it risk drowning.

## 6. Data Availability

The data analyzed in this submission are available at Zenodo: <https://doi.org/10.5281/zenodo.4059885>

## 7. Author Contribution

MI designed and performed the model simulations, RGB assisted with model setup. MI wrote the manuscript with feedback and guidance from LJM, PR, SDH, RGB. All authors provided feedback and guidance on the project. LJM supervised the project.

## 8. Competing Interests

The authors declare that they have no conflict of interest.



## 9. Acknowledgements

360 This work was funded by the US National Oceanic and Atmospheric Association (NOAA) via the NOS/NCCOS/CRP Ecological Effects of Sea-Level Rise Program (grant no. NA15NOS4780172) to P.R., S.D.H., and L.J.M as well as the Preston Jones and Mary Elizabeth Frances Dean Martin Fellowship Fund, and by the Virginia Coast Reserve Long-Term Ecological Research Program (National Science Foundation DEB-1832221) via a subaward to the University of North Carolina at Chapel Hill.

## 365 References:

- Anthony, E. J., Vanhee, S., & Ruz, M. H. (2007). An assessment of the impact of experimental brushwood fences on foredune sand accumulation based on digital elevation models. *Ecological Engineering*, 31(1), 41–46. <https://doi.org/10.1016/j.ecoleng.2007.05.005>
- Biel, R. G., Hacker, S. D., Ruggiero, P., Cohn, N., & Seabloom, E. W. (2017). Coastal protection and conservation on sandy beaches and dunes: Context-dependent tradeoffs in ecosystem service supply. *Ecosphere*, 8(4). <https://doi.org/10.1002/ecs2.1791>
- Biel, R. G., Hacker, S. D., & Ruggiero, P. (2019). Elucidating coastal foredune ecomorphodynamics in the US Pacific Northwest via Bayesian networks. *Journal of Geophysical Research: Earth Surface*, (In Press). <https://doi.org/10.1029/2018JF004758>
- 375 Brodie, K., Conery, I., Cohn, N., Spore, N., & Palmsten, M. (2019). Spatial Variability of Coastal Foredune Evolution, Part A: Timescales of Months to Years. *Journal of Marine Science and Engineering*, 7(5), 1–28. <https://doi.org/10.3390/jmse7050124>
- Charbonneau, B. R., & Wnek, J. P. (2016). Reactionary fence installation for post-Superstorm Sandy dune recovery. *Shore and Beach*, 84(3), 42–48.
- 380 Duran, O., & Moore, L. J. (2013). Vegetation controls on the maximum size of coastal dunes. *Proceedings of the National Academy of Sciences*, 110(43), 17217–17222. <https://doi.org/10.1073/pnas.1307580110>
- Durán, R., Guillén, J., Ruiz, A., Jiménez, J. A., & Sagristà, E. (2016). Morphological changes, beach inundation and overwash caused by an extreme storm on a low-lying embayed beach bounded by a dune system (NW Mediterranean). *Geomorphology*, 274, 129–142. <https://doi.org/10.1016/j.geomorph.2016.09.012>
- 385 Elko, N., Brodie, K., Stockdon, H., Nordstrom, K., Houser, C., Mckenna, K., et al. (2016). Dune management challenges on developed coasts. *Shore and Beach*, 84(1), 1–14.



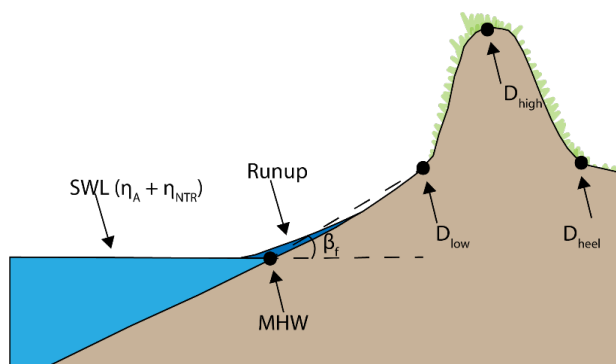
- Goldstein, E. B., Mullins, E. V., Ruggiero, P., Hacker, S. D., Brown, J. K., Biel, R. G., et al. (2018). Literature-based latitudinal distribution and possible range shifts of two US east coast dune grass species ( *Uniola paniculata* and *Ammophila breviligulata* ). *PeerJ*, 6, e4932. <https://doi.org/10.7717/peerj.4932>
- 390 Hacker, S. D., Zametske, P., Seabloom, E., Ruggiero, P., Mull, J., Gerrity, S., & Jones, C. (2012). Subtle differences in two non-native congeneric beach grasses significantly affect their colonization, spread, and impact. *Oikos*, 121(1), 138–148. <https://doi.org/10.1111/j.1600-0706.2011.18887.x>
- Hacker, S. D., Jay, K. R., Cohn, N., Goldstein, E. B., Hovenga, P. A., Itzkin, M., et al. (2019). Species-Specific Functional Morphology of Four US Atlantic Coast Dune Grasses : Biogeographic Implications for Dune Shape and Coastal Protection. *Diversity*, 11, 1–16. <https://doi.org/10.3390/d11050082>
- 395 Itzkin, M., Moore, L. J., Ruggiero, P., & Hacker, S. D. (2020). The effect of sand fencing on the morphology of natural dune systems. *Geomorphology*, 352, 106995. <https://doi.org/10.1016/j.geomorph.2019.106995>
- Jackson, N. L., & Nordstrom, K. F. (2018). Aeolian sediment transport on a recovering storm-eroded foredune with sand fences. *Earth Surface Processes and Landforms*, 43(6), 1310–1320. <https://doi.org/10.1002/esp.4315>
- 400 Larson, M., Erikson, L., & Hanson, H. (2004). An analytical model to predict dune erosion due to wave impact. *Coastal Engineering*, 51(8–9), 675–696. <https://doi.org/10.1016/j.coastaleng.2004.07.003>
- Leatherman, S. P. (1979). Migration of Assateague Island, Maryland, by inlet and overwash processes. *Geology*, 7(2), 104–107.
- Long, J. W., de Bakker, A. T. M., & Plant, N. G. (2014). Scaling coastal dune elevation changes across storm-impact regimes. *Geophysical Research Letters*, 41(8), 2899–2906. <https://doi.org/10.1002/2014GL059616>
- 405 Lorenzo-Trueba, J., & Ashton, A. D. (2014). Rollover, drowning, and discontinuous retreat: Distinct modes of barrier response to sea-level rise arising from a simple morphodynamic model. *Journal of Geophysical Research: Earth Surface*, 119(4), 779–801. <https://doi.org/10.1002/2013JF002941>
- Magliocca, N. R., McNamara, D. E., & Murray, A. B. (2011). Long-Term, Large-Scale Morphodynamic Effects of Artificial Dune Construction along a Barrier Island Coastline. *Journal of Coastal Research*, 27(5), 918–930. <https://doi.org/10.2112/JCOASTRES-D-10-00088.1>
- 410 Mendelssohn, I. A., Hester, M. W., Monteferrante, F. J., Journal, S., Winter, N., Mendelssohn, I. A., et al. (1991). Experimental Dune Building and Vegetative Stabilization in a Sand-Deficient Barrier Island Setting on the Louisiana Coast , USA. *Journal of Coastal Research*, 7(1), 137–149.



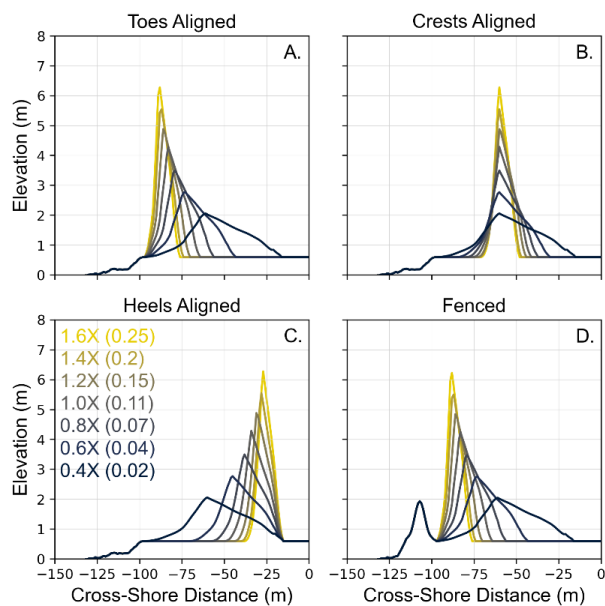
- 415 Miller, D. L., Thetford, M., & Yager, L. (2001). Evaluation of Sand Fence and Vegetation for Dune Building following  
Overwash by Hurricane Opal on Santa Rosa Island, Florida. *Journal of Coastal Research*, 17(4), 936–948.  
Retrieved from <http://www.jstor.org/stable/4300253>
- Mull, J., & Ruggiero, P. (2014). Estimating Storm-Induced Dune Erosion and Overtopping along U.S. West Coast  
Beaches. *Journal of Coastal Research*, 30(6), 1173–1187. <https://doi.org/10.2112/JCOASTRES-D-13-00178.1>
- 420 Mullins, E., Moore, L. J., Goldstein, E. B., Jass, T., Bruno, J., & Durán Vinent, O. (2019). Investigating dune-building  
feedback at the plant level: Insights from a multispecies field experiment. *Earth Surface Processes and  
Landforms*, 0–2. <https://doi.org/10.1002/esp.4607>
- Nordstrom, K. F., & Jackson, N. L. (2013). Foredune restoration in urban settings. In M. L. Martinez (Ed.), *Restoration  
of Coastal Dunes* (pp. 17–31). Springer-Verlag Berlin Heidelberg. [https://doi.org/10.1007/978-3-642-33445-](https://doi.org/10.1007/978-3-642-33445-0_2)  
425 [0\\_2](https://doi.org/10.1007/978-3-642-33445-0_2)
- Nordstrom, K. F., Lampe, R., & Vandemark, L. M. (2000). Reestablishing naturally functioning dunes on developed  
coasts. *Environmental Management*, 25(1), 37–51. <https://doi.org/10.1007/s002679910004>
- Nordstrom, K. F., Jackson, N. L., Freestone, A. L., Korotky, K. H., & Puleo, J. A. (2012). Effects of beach raking and  
sand fences on dune dimensions and morphology. *Geomorphology*, 179, 106–115.  
430 <https://doi.org/10.1016/j.geomorph.2012.07.032>
- Roelvink, D., Reniers, A., van Dongeren, A., van Thiel de Vries, J., McCall, R., & Lescinski, J. (2009). Modelling  
storm impacts on beaches, dunes and barrier islands. *Coastal Engineering*, 56(11–12), 1133–1152.  
<https://doi.org/10.1016/j.coastaleng.2009.08.006>
- Roelvink, D., McCall, R., Mehvar, S., Nederhoff, K., & Dastgheib, A. (2018). Improving predictions of swash  
435 dynamics in XBeach: The role of groupiness and incident-band runup. *Coastal Engineering*, 134(February  
2017), 103–123. <https://doi.org/10.1016/j.coastaleng.2017.07.004>
- Rogers, L. J., Moore, L. J., Goldstein, E. B., Hein, C. J., Lorenzo-Trueba, J., & Ashton, A. D. (2015). Anthropogenic  
controls on overwash deposition: Evidence and consequences. *Journal of Geophysical Research: Earth Surface*,  
120(12), 2609–2624. <https://doi.org/10.1002/2015JF003634>
- 440 Ruggiero, P., Holman, R. A., & Beach, R. A. (2004). Wave run-up on a high-energy dissipative beach. *Journal of  
Geophysical Research: Oceans*, 109(6), 1–12. <https://doi.org/10.1029/2003JC002160>
- Sallenger, A. H. (2000). Storm Impact Scale for Barrier Islands. *Journal of Coastal Research*, 16(3), 890–895.



- <https://doi.org/10.2307/4300099>
- Seabloom, E. W., Ruggiero, P., Hacker, S. D., Mull, J., & Zarnetske, P. (2013). Invasive grasses, climate change, and exposure to storm-wave overtopping in coastal dune ecosystems. *Global Change Biology*, *19*(3), 824–832. <https://doi.org/10.1111/gcb.12078>
- Serafin, K. A., & Ruggiero, P. (2014). Simulating extreme total water levels using a time-dependent, extreme value approach. *Journal of Geophysical Research: Oceans*, *119*, 6305–6329. <https://doi.org/10.1002/2014JC010093>. Received
- Stockdon, H. F., Holman, R. A., Howd, P. A., & Sallenger, A. H. (2006). Empirical parameterization of setup, swash, and runup. *Coastal Engineering*, *53*(7), 573–588. <https://doi.org/10.1016/j.coastaleng.2005.12.005>
- Stockdon, H. F., Sallenger, A. H., Holman, R. A., & Howd, P. A. (2007). A simple model for the spatially-variable coastal response to hurricanes. *Marine Geology*, *238*(14), 1–20. <https://doi.org/10.1016/j.margeo.2006.11.004>
- Stockdon, H. F., Doran, K. J., Thompson, D. M., Sopkin, K. L., & Plant, N. G. (2013). *National Assessment of Hurricane-Induced Coastal Erosion Hazards: Southeast Atlantic Coast. U.S. Geological Survey Open-File Report*. <https://doi.org/http://dx.doi.org/10.3133/ofr20141243>
- Straub, J. A., Rodriguez, A. B., Luettich, R. A., Moore, L. J., Itzkin, M., Ridge, J. T., et al. (2020). The role of beach state and the timing of pre-storm surveys in determining the accuracy of storm impact assessments. *Marine Geology*, *425*(April), 1–14. <https://doi.org/10.1016/j.margeo.2020.106201>
- Woodhouse, W. W., Seneca, E. D., & Broome, S. W. (1977). Effect of species on dune grass growth. *International Journal of Biometeorology*, *21*(3), 256–266. <https://doi.org/10.1007/BF01552879>
- Zarnetske, P. L., Seabloom, E. W., & Hacker, S. D. (2010). Non-target effects of invasive species management: beachgrass, birds, and bulldozers in coastal dunes. *Ecosphere*, *1*(5), Article 13. <https://doi.org/10.1890/ES10-00101.1>
- Zarnetske, P. L., Hacker, S. D., Seabloom, E. W., Ruggiero, P., Killian, J. R., Maddux, T. B., & Cox, D. (2012). Biophysical Feedback Mediates Effects of Invasive Grasses on Coastal Dune Shape. *Ecology*, *93*(6), 1439–1450. <https://doi.org/10.1890/11-1112.1>



475 **Figure 1: Schematic beach and dune profile showing the dune toe ( $D_{low}$ ), crest ( $D_{high}$ ), and heel ( $D_{heel}$ ), beach slope ( $\beta_f$ ), mean high water contour (MHW), still water level (SWL) and runup, modified from Sallenger (2000).**



480 **Figure 2: Synthetic dune profiles; (A) dune toes aligned, (B) dune crests aligned, (C) dune heels aligned, and (D) fenced dune included. The proportional change in aspect ratio (i.e., dune height divided by width) relative to the reference profile (1.0x) is shown in panel C (aspect ratio in parentheses).**

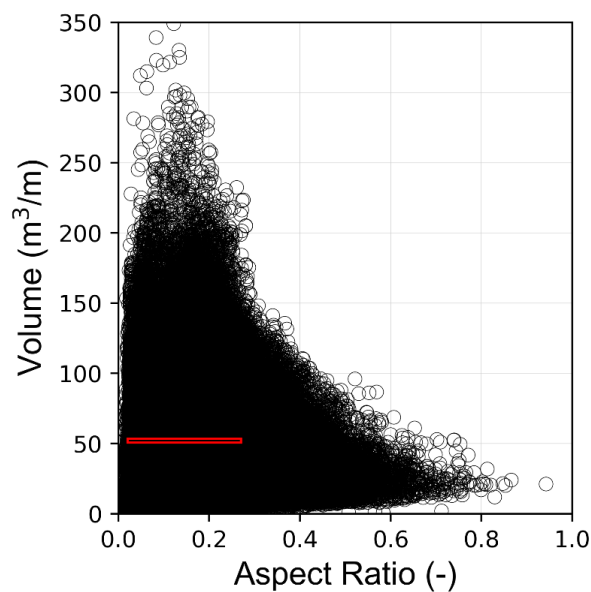
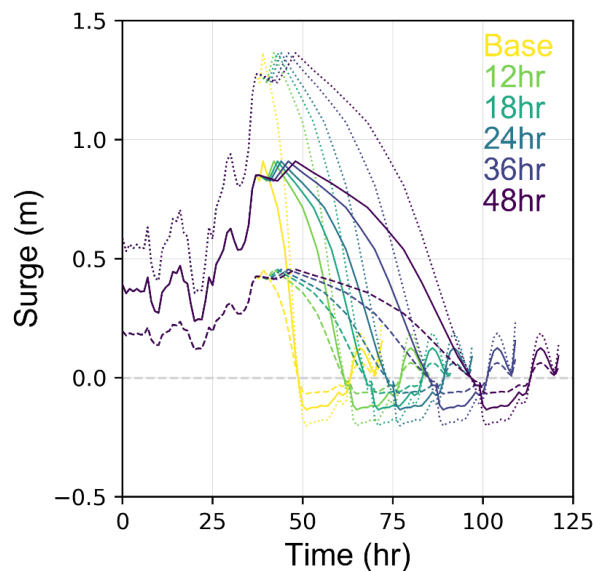
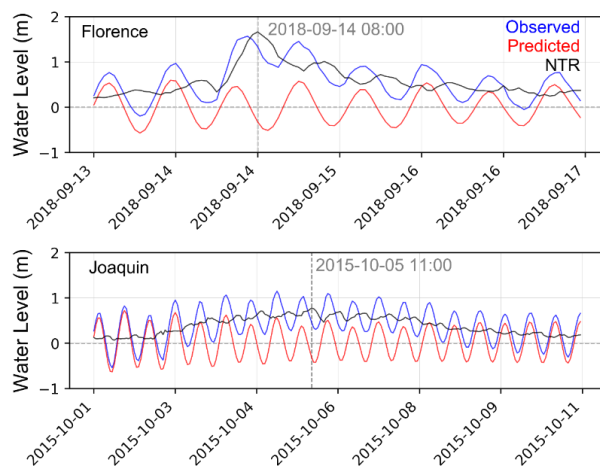


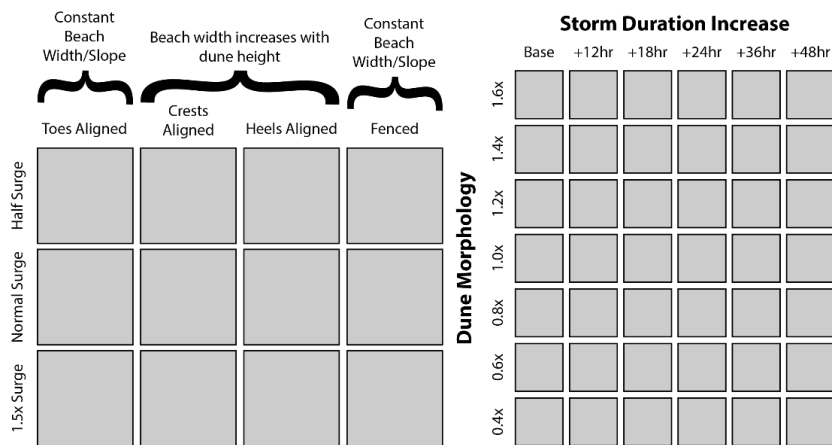
Figure 3: Dune volume versus dune aspect ratio measured from LiDAR profiles from Bogue Banks, NC, USA, collected between 1997-2016. The red box represents the range of conditions simulated in this study.



485 Figure 4: Synthetic storm surge time series used in this study. Colors refer to the storm duration increase. Dashed lines represent the 0.5x surge, solid lines represent the 1.0x surge, and dotted lines represent the 1.5x surge.



490 **Figure 5: Hydrographs for Hurricane Florence (top) and Tropical Storm Joaquin (bottom) showing observed water levels (blue), predicted water levels (red), and the non-tidal residual (NTR, black). The timing of peak surge for each storm is highlighted by the vertical dashed line.**



495 **Figure 6: Schematic overview of XBeach simulations. For every combination of storm intensity and dune alignment shown in the left matrix (12 total), we ran every combination of dune shape and storm duration shown in the right matrix (42 total).**

500

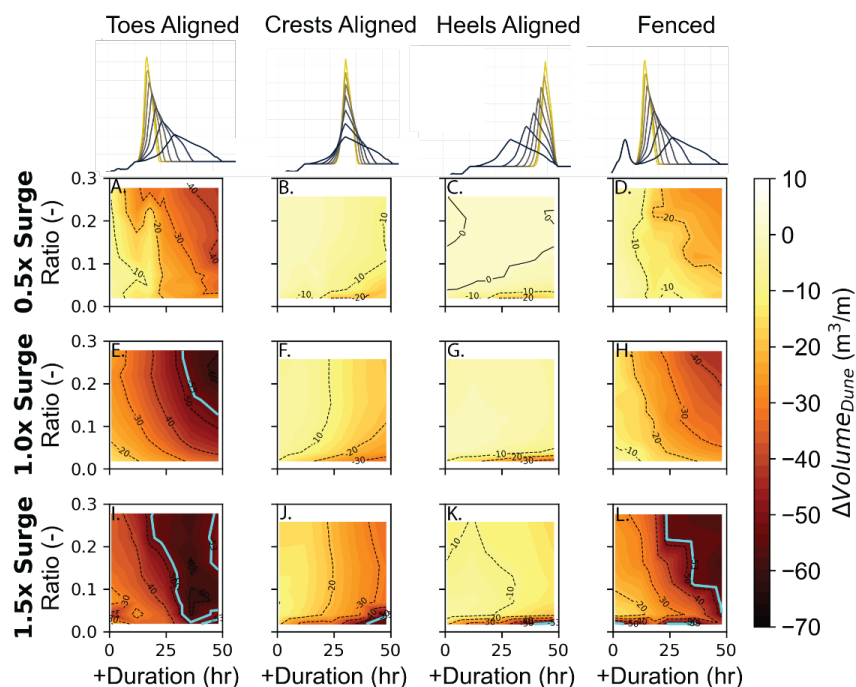
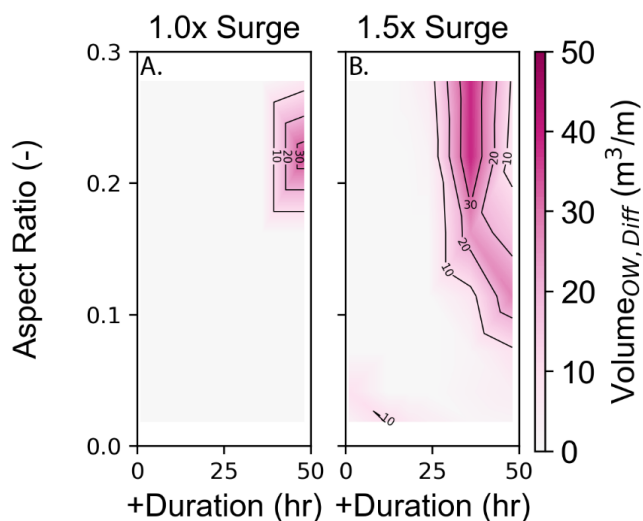
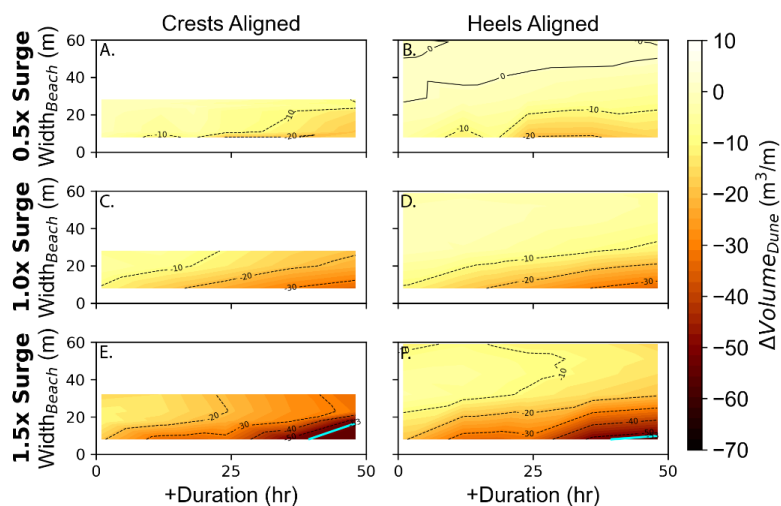


Figure 7: Dune aspect ratio versus storm duration for all simulations. Color depicts change in dune volume. Each row of plots represents a different storm intensity (increasing from top to bottom) and each column of plots represents a different dune configuration. Highlighted regions (cyan line) indicate simulations where the foredune was inundated (low aspect ratio) or laterally eroded (high aspect ratio).

505



510 **Figure 8: The difference in dune overwash volumes for the equivalent dune simulations with and without fences. Darker colors indicate a greater overwash volume for the non-fenced simulation.**



515 **Figure 9: Beach width versus storm duration for dune simulations, colored by the change in dune volume, similar to Figure 7 but with the y-axis re-scaled based on the initial beach width in each simulation. Each row of plots represents a different storm intensity (increasing from top to bottom) and each column of plots represents a different dune configuration. Because simulations for the dune toes-aligned and the fenced dunes do not have any variation in the beach width, they are not included in this analysis. Highlighted regions (cyan**  
 520 **line) indicate where the dunes were inundated.**

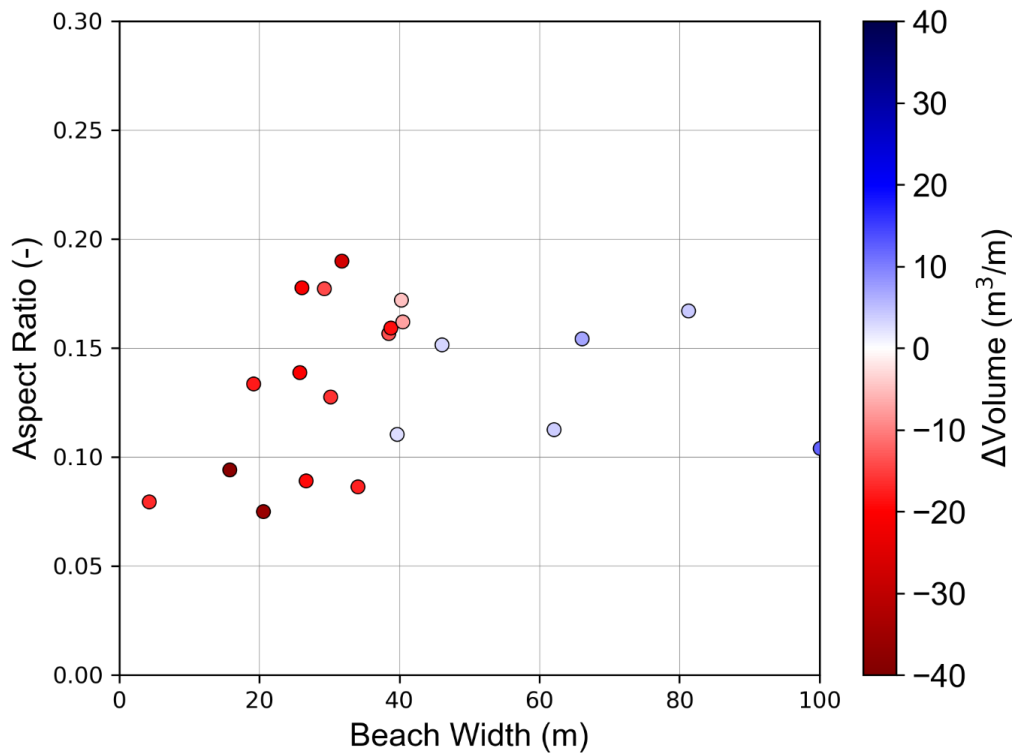


Figure 10. Pre-storm aspect ratio versus pre-storm beach width for foredunes at Bogue Banks, NC. Each point represents a transect and points are colored based on the change in volume from 2017-2018.

525